IEEE Access
Multidisciplinary ⋮ Rapid Review ⋮ Open Access Journal

Received January 10, 2022, accepted January 19, 2022, date of publication January 26, 2022, date of current version February 10, 2022.

Digital Object Identifier 10.1109/ACCESS.2022.3146417

Model-Free Geometric Fault Detection and Isolation for Nonlinear Systems Using Koopman Operator

MOHAMMADHOSEIN BAKHTIARIDOUST[1], MEYSAM YADEGAR[1], NADER MESKIN[2], (Senior Member, IEEE), AND MOHAMMAD NOORIZADEH[2]

[1]Department of Electrical and Computer Engineering, Qom University of Technology, Qom 1519-37195, Iran
[2]Department of Electrical Engineering, Qatar University, Doha, Qatar

Corresponding author: Nader Meskin (nader.meskin@qu.edu.qa)

This work was supported by Open Access funding provided by the Qatar National Library.

ABSTRACT This paper presents a model-free fault detection and isolation (FDI) method for nonlinear dynamical systems using Koopman operator theory and linear geometric technique. The key idea is to obtain a Koopman-based reduced-order model of a nonlinear dynamical system and apply the linear geometric FDI method to detect and isolate faults in the system. Koopman operator is an infinite-dimensional, linear operator which lifts the nonlinear dynamic data into an infinite-dimensional space where the correlations of dynamic data behave linearly. However, due to the infinite dimensionality of this operator, an approximation of the operator is needed for practical purposes. In this work, the Koopman framework is adopted toward nonlinear dynamical systems in combination with the linear geometric approach for fault detection and isolation. In order to demonstrate the efficacy of the proposed FDI solution, a mathematical nonlinear dynamical system, and an experimental three-tank setup are considered. Results show a remarkable performance of the proposed geometric Koopman-based fault detection and isolation (K-FDI) technique.

INDEX TERMS Model-free fault detection and isolation, Koopman operator, extended dynamic mode decomposition, geometric approach, reduced-order model.

I. INTRODUCTION

The issues of reliability, operating safety, availability, and environmental protection concerns in modern control systems have become significantly important and received more attention during recent years since faults may result in irreparable consequences for the safe and efficient operation of the system. This gives rise to demands for research on fault detection and isolation (FDI) approaches. The term ''fault'' simply means any unexpected deviation of system function that disturbs the system's normal operation [1]. Fault detection evaluates whether a fault has occurred or the system is operating under a normal condition. On the other hand, fault isolation methods locate and isolate the cause of the fault [2]. FDI methods can be broadly classified as *model-based* and *model-free* [3].

In the model-based approaches, the analytical model of the underlying dynamical system is considered for designing FDI algorithms [4], [5]. In case of linear models, model-based techniques basically have been categorized as *observer-based*, *parity equation*, and *parameter estimation* methods [6]. The observer-based approach itself divides into *deterministic* [7] and *stochastic* [8] settings where the Luenberger observers and Kalman filters are used for estimating the system's output from the measurements (or subset of measurement) for each, respectively. In these approaches, the weighted output estimation error is used as a residual. In the parity space approach, the residual signals are generated based upon consistency checks on system input and output data over a given time window [9]. The main idea in the parameter estimation method is an online estimation of the actual system parameters using the well-known parameter estimation schemes and comparing them with the reference model parameters [10].

In addition to the approaches for linear systems, the design and analysis of FDI schemes for nonlinear systems have also received more attention in recent years [11]. Unlike linear systems, these techniques are only applicable to certain

The associate editor coordinating the review of this manuscript and approving it for publication was Francesco Tedesco.

classes of nonlinearity. These methods are mostly the extension of linear model-based approaches. In [12], the unknown input observer was extended to include nonlinearity. Furthermore, an extension of the parity space was developed in [13] for some classes of non-linear systems and [14] derives the parity vectors that construct optimized residual generators for linear and nonlinear systems. Sliding mode observers have been designed in [15] for non-linear FDI.

Meanwhile, the geometric approach plays an important role in investigating the problem of fault detection and isolation for a wide range of dynamical systems such as LTI systems [16], Markovian jump systems [17], [18], LPV systems [19], linear impulsive systems [20], time-delay systems [21], multi-dimensional systems [22], and parabolic PDE systems [23]. Furthermore, a geometric approach for the problem of nonlinear FDI is proposed in [24]. The geometric approach provides necessary and sufficient conditions that allow for designing a residual generator, only sensitive to certain faults in the system. Generally, the main drawback of the model-based approaches is that all of the techniques require a precise mathematical model of the system under supervision while obtaining an accurate model is very hard for many practical systems [25].

The difficulty of capturing systems complexities in first principal models and the ability to collect a huge amount of data from the system with the help of the smart industries and digital communication have contributed to the rapid development of model-free methods [26]. Since model-free methods use soft-computing techniques, in some literature, they have been referred to as soft-computing-based methods as well [6]. Model-free methods can be classified as *qualitative* such as fuzzy [27] and *quantitative* like neural network [28] and evolutionary algorithm [29]. Although artificial intelligence-based methods are strong in detecting faults, these methods have two main downsides. First, they do not provide a meaningful representation of the underlying dynamics, which does not let the analytical analysis of the system. Next, they rely on classifiers for fault isolation, which requires faulty data to train the classifiers. On the other hand, although several strong techniques have been developed for model-based FDI, they are not helpful in model-free schemes since they need an analytical model of the plant.

An alternative data-driven approach that provides meaningful insight into the dynamics of the underlying system is through the Koopman operator. This linear, infinite-dimensional operator describes the temporal evolution of observable functions. A finite-dimensional approximation of the Koopman operator has been applied to various control applications [30]–[34]. In [35], a data-driven Koopman-based method is proposed for the machinery health monitoring and prediction problem of noisy industrial signals. Furthermore, the anomaly detection framework based on using Koopman model forms along with classical linear systems and control approaches is presented in [36] and used to detect faults in power grid applications.

In this paper, a novel model-free approach for fault detection and isolation of nonlinear dynamical systems is proposed using the linear geometric technique by adopting the Koopman operator perspective toward dynamical systems. The linear Koopman preditor obtained by a finite-approximation of the operator serves as an equivalent linear model of the underlying nonlinear dynamics in the whole operating region with the same input-output characteristics as the nonlinear dynamics. The work in [35] only develops a new DMD-based approach for dealing with noisy low dimensional data along with Koopman mode for fault detection and the remaining useful life estimation; hence it is different from the FDI framework developed in this paper. This work is different from the one in [36], where the current work offers both detection and isolation of the faults for nonlinear systems with actuation, but in [36] only the detection scheme for the autonomous system is adopted. This work differs from the method in [14], where [14] only focuses on detecting the fault and is limited to a particular class of nonlinear systems modeled via Hammerstein models. At the same time, the proposed Koopman framework considers isolating the fault in addition to detection and is valid for general nonlinear dynamics. Unlike model-free methods mentioned earlier, this method provides a meaningful representation of the underlying dynamic, capturing its inherent properties and allowing conducting an analytical analysis and design. Using the reduced-order modeling techniques, a Koopman-based reduced order model (K-ROM) [37] of the underlying system is obtained, and then the FDI geometric approach is used for fault detection and isolation of nonlinear dynamical systems. The key features of the proposed FDI framework are as follows:

1) Although it is possible to treat nonlinear FDI linearly using linearization, one needs to estimate the parameters of the corresponding linearized system around each operating point, and solutions are only valid locally [38]. In the presented method, however, by incorporating the Koopman operator in an FDI framework, one can use linear model-based techniques to treat the nonlinear FDI problem linearly, and the solution is valid globally due to the global characteristics of the Koopman operator.
2) Model-based FDI approaches are well-developed and are easy to implement. However, the problem with these methods is that they require an accurate mathematical model of the underlying dynamics. Since the proposed method approximates the Koopman operator from data using an extended DMD (EDMD) [39] scheme, the method is entirely data-driven; hence no knowledge about the underlying dynamic is needed.
3) There are statistical and artificial intelligence FDI methods like PCA-based methods [40], and neural network-based methods [41], that do not need any knowledge of the dynamics. These methods do not provide a meaningful representation of the system and

do not let analytical analysis. Furthermore, to isolate the fault, they rely on classifiers. These classifiers need faulty data in their training phase to perform proper fault isolation. The proposed method obtains an interpretable and meaningful representation of the nonlinear dynamics by estimating the Koopman predictors. This system representation will lead to designing the observers for fault isolation without needing any faulty data to train any classifiers. Hence, the proposed method only relies on the system's healthy data obtained during the system's normal operation for FDI.

To summarize, the main contribution of the paper is to develop a data-driven FDI approach where the structural properties of the system are captured through the Koopman approximation. Then, the geometric FDI approach is applied to K-ROM for performing fault detection and isolation. In other words, in our proposed FDI solution, the integration of Koopman theory, dynamic mode decomposition, and linear geometric framework lead to a data-driven FDI methodology, which merges the advantages of model-based and model-free FDI techniques in a unified framework.

The remainder of the paper is organized as follows. The review of the basic geometric concepts and the geometric approach to the FDI problem are presented in Section II. Section III introduces the Koopman operator theory and describes the numerical approximation of that operator. In Section IV, the design procedure of the proposed Koopman-based linear residual generator for nonlinear dynamical systems is presented. In Section V, the effectiveness of the proposed K-FDI method is verified by a numerical example, and a comparative study is investigated. In Section VI the proposed method is validated by an experimental case study. Finally, the paper ends with a conclusion in Section VII.

II. GEOMETRIC FAULT DETECTION AND ISOLATION

In this section, a FDI geometric approach is presented which is indeed the problem of designing a residual signal only sensitive to certain faults using a geometric perspective. We refer the reader to [42] for more concrete discussions on the geometric mathematics. Consider a discrete-time system written as

$$\begin{aligned} x(k+1) &= Ax(k) + Bu(k) + \sum_{i=1}^{M} L_i f_i(k), \\ y(k) &= Cx(k), \end{aligned} \tag{1}$$

where $x \in \mathcal{X} \subset \mathbb{R}^n$ is the state, $u \in \mathcal{U} \subset \mathbb{R}^q$ is the control input, $y \in \mathcal{Y} \subset \mathbb{R}^l$ the system output, $f_i \in \mathbb{R}^{M_i}$, $i \in \boldsymbol{M}$, are the fault modes and L_i, $i \in \boldsymbol{M}$, are the fault signatures where $\boldsymbol{M}$ denotes a finite set $\{1, 2, \ldots, M\}$.

Definition 1 (Invariant Subspaces [42]): Consider a linear map $A : \mathcal{X} \to \mathcal{X}$, then a subspace $\mathcal{S} \subseteq \mathcal{X}$ is said to be an A-invariant if $A\mathcal{S} \subseteq \mathcal{S}$.

The null space of a linear map $C : \mathcal{X} \to \mathcal{Y}$ is denoted by $\ker C$ and the largest A-invariant subspace contained in $\ker C$ is then defined as

$$\langle \ker C | A \rangle \triangleq \bigcap_{z=0}^{n-1} \ker CA^z. \tag{2}$$

Definition 2 (Conditioned Invariant Subspace [42]): A subspace $\mathcal{S} \subseteq \mathcal{X}$ is said to be (A, C)-conditioned invariant if and only if there exists a matrix D such that

$$(A + DC)\mathcal{S} \subseteq \mathcal{S}. \tag{3}$$

Let $\underline{D}(\mathcal{S})$ denote the class of all maps $D : \mathcal{Y} \to \mathcal{X}$ such that (3) holds. One can compute the minimum (A, C)-conditioned invariant containing $\mathcal{L} \subseteq \mathcal{X}$ denoted by $\mathcal{W}^*(\mathcal{L})$ using a recursive algorithm where $\mathcal{W}^*(\mathcal{L}) = \lim_{z \to n} \mathcal{W}^z$ is given by

$$\begin{aligned} \mathcal{W}^{z+1} &= \mathcal{L} + A(\mathcal{W}^z \cap \ker C), \\ \mathcal{W}^0 &= 0. \end{aligned} \tag{4}$$

Definition 3 (Unobservability Subspaces [43]): A subspace $\mathcal{S} \subseteq \mathcal{X}$, is an unobservability subspace (u.o.s) for system (1) if

$$\mathcal{S} = \langle \ker HC | A + DC \rangle, \tag{5}$$

where $H : \mathcal{Y} \to \mathcal{Y}$ is a measurement mixing.
Let us denote the class of all unobservability subspaces containing $\mathcal{L}$ by $\underline{\mathcal{S}}(\mathcal{L})$. Also one can compute the minimum unobservability subspace containing $\mathcal{L} \subseteq \mathcal{X}$ denoted by $\mathcal{S}^*(\mathcal{L})$ where $\mathcal{S}^*(\mathcal{L}) = \lim_{z \to n} \mathcal{S}^z$ is given by

$$\begin{aligned} \mathcal{S}^{z+1} &= \mathcal{W}^* + (A^{-1}\mathcal{S}^z) \cap \ker C, \\ \mathcal{S}^0 &= \mathcal{X}. \end{aligned} \tag{6}$$

Since sensor fault can also be modeled as pseudo-actuator faults, it is assumed that for sensor faults, A, B and the fault modes have been modified accordingly [16].

Now by denoting $\Omega_j \subseteq \boldsymbol{M}, j \in \boldsymbol{N}$, as the coding set, the FDI filter problem is the design of an LTI residual generator that takes u and y as input and generates a set of residual vectors r_i, $i \in \boldsymbol{N}$, such that (I) when no fault is present, all the generated residuals r_i decay asymptotically to zero, and (II) the j'th component fault only affect the residuals r_i for $i \in \Omega_j$, i.e., other residuals r_a for $a \in \boldsymbol{N} - \Omega_j$, are decoupled from this fault [16]. For this purpose, a predetermined family of coding sets should be chosen so that by knowing which of the r_i are zero and which are not, one can be able to identify the failure uniquely. One of the commonly used coding set is to use so-called *dedicated residual set* [1], i.e., $\Omega_i = \{i\}$, and $N = M$.

The fundamental problem of residual generation (FPRG) is a simplified version of the FDI filter problem. In this problem, the system given by (1) is considered with only two failure events present, i.e., $M = 2$, and the goal is to design a residual generator sensitive to the first fault and not to the second one. The solvability condition of FPRG is stated in the following theorem.

Lemma 1 [16]: FPRG has a solution if and only if $\mathcal{S}^*(\mathcal{L}_2) \cap \mathcal{L}_1 = 0$ where $\mathcal{S}^*(\mathcal{L}_2)$ is the infimal element of $\underline{\mathcal{S}}(\mathcal{L}_2)$ and $\mathcal{L}_i = \mathrm{Im}(L_i)$.

This can be easily extended to the case where $M > 2$, also known as extended FPRG [16].

III. KOOPMAN BASED IDENTIFICATION FOR ACTUATED SYSTEM

A. KOOPMAN OPERATOR THEORY

In this section, to provide some background for the approach, the Koopman operator theory is briefly reviewed for autonomous discrete-time nonlinear systems with no actuation. Then, the generalization of the Koopman operator to the systems with exogenous inputs is considered.

1) KOOPMAN OPERATOR-NO INPUT

Consider a discrete-time nonlinear system of the form

$$x(k+1) = f(x(k)), \tag{7}$$

where the state $x \in \mathcal{X} \subset \mathbb{R}^n$, and $f : \mathcal{X} \to \mathcal{X}$. Next, a set of output functions can be defined as $g : \mathcal{X} \to \mathbb{R}$ which will be often referred to as *observable functions*. Now, the Koopman operator is defined as $\mathcal{K} : \mathcal{F} \to \mathcal{F}$ where $\mathcal{F}$ is a Banach space of observable functions $g : \mathcal{X} \to \mathbb{R}$ associated with the mapping function $f : \mathcal{X} \to \mathcal{X}$ as

$$\mathcal{K}g(x) \triangleq g(f(x)). \tag{8}$$

Note that the space of observable functions $\mathcal{F}$ should be closed under the action of the operator $\mathcal{K}$. Having a linear operator $\mathcal{K}$ since

$$\mathcal{K}(c_1 g_1 + c_2 g_2) = c_1 \mathcal{K} g_1 + c_2 \mathcal{K} g_2, \tag{9}$$

the eigen-value problem for that can be written as

$$\mathcal{K}\varphi_j(x) = \lambda_j \varphi_j(x), \ j = 1, 2, \ldots, \infty. \tag{10}$$

By taking the Koopman eigen-functions as a basis for the space $\mathcal{F}$, one can expand each of the observable functions on this basis as

$$g_i(x) = \sum_{j=1}^{\infty} v_{ij} \varphi_j(x). \tag{11}$$

By considering vector-valued

$$\boldsymbol{g}(x) = \begin{bmatrix} g_1(x) & g_2(x) & \cdots & g_p(x) \end{bmatrix}^T, \tag{12}$$

we can similarly expand the vector of observable functions as

$$\boldsymbol{g}(x) = \sum_{j=1}^{\infty} \varphi_j(x) \boldsymbol{v}_j, \tag{13}$$

where the coefficients $\boldsymbol{v}_j$ are the *Koopman modes* related to $\boldsymbol{g}$. Although Koopman is a linear operator but since it acts on functions, this operator is *infinite*-dimensional which makes it hard for representation. The *Koopman invariant subspace* as introduced in [44] is a subspace given by the span of the set $\{\psi\}_{i=1}^{M}$ if all functions g in this subspace, i.e.,

$$g = \alpha_1 \psi_1 + \alpha_2 \psi_2 + \ldots + \alpha_p \psi_p, \tag{14}$$

remain in this subspace after being acted by the operator $\mathcal{K}$:

$$\mathcal{K}g = \beta_1 \psi_1 + \beta_2 \psi_2 + \ldots + \beta_p \psi_p. \tag{15}$$

Koopman eigen-functions will provide us such invariant subspace, and by restricting the operator to it, one can obtain a finite-dimensional representation of the operator $\mathcal{K}$.

2) KOOPMAN OPERATOR-WITH INPUT

Consider a discrete-time nonlinear system with inputs

$$x(k+1) = f(x(k), u(k)), \tag{16}$$

where the state $x \in \mathcal{X}$, the control $u \in \mathcal{U}$, and the vector field $f : \mathcal{X} \times \mathcal{U} \to \mathcal{X}$. As in [39], an extended state space can be defined as the product of the space of original states and the space of all control sequences. Then, consider the Koopman operator associated to (16) as the Koopman operator evolving the extended state variable defined as

$$X_e \triangleq \begin{bmatrix} x \\ \mathbf{u} \end{bmatrix}, \tag{17}$$

where $\mathbf{u} \triangleq (u(i))_{i=0}^{\infty}$ is the sequence with $u(i) \in \mathcal{U}$, $\mathcal{R}(\mathcal{U})$ is the space of all sequences $\mathbf{u}$, and $X_e \in \mathcal{X} \times \mathcal{R}(\mathcal{U})$. Then, the dynamics of X_e is described as

$$X_e(k+1) = f_e(X_e(k)) \triangleq \begin{bmatrix} f(x(k), \mathbf{u}(0)) \\ \mathcal{S}_l \mathbf{u} \end{bmatrix}, \tag{18}$$

where $\mathbf{u}(0)$ is the first element of the sequence $\mathbf{u}$, and $\mathcal{S}_l$ is the left shift operator:

$$(\mathcal{S}_l \mathbf{u})(i) = \mathbf{u}(i+1). \tag{19}$$

The Koopman operator $\mathcal{K} : \mathcal{H} \to \mathcal{H}$ associated to (18) is defined by

$$\mathcal{K}\Phi(X_e) \triangleq \Phi(f_e(X_e)), \tag{20}$$

where $\Phi : \mathcal{X} \times \mathcal{R}(\mathcal{U}) \to \mathbb{R}$ is the extended observable function and $\mathcal{H}$ is the extended observable function space.

B. NUMERICAL APPROXIMATION OF KOOPMAN OPERATOR

Since the Koopman operator is an infinite dimensional operator, in practice, obtaining a finite dimensional approximation of this operator is necessary. Assume that we can measure the full state of the system. We collect the snapshots of data $x(k), k = 1, \ldots, m+1$, from the dynamical system and form the matrices X and X' as

$$X = \begin{bmatrix} x(1) & x(2) & \ldots & x(m) \end{bmatrix}, \tag{21}$$

$$X' = \begin{bmatrix} x(2) & x(3) & \ldots & x(m+1) \end{bmatrix}, \tag{22}$$

where X and X' are both in $\mathbb{R}^{n \times m}$. Now by using DMD algorithm [45], one can obtain the best fit linear operator in the least square sense as $A = X' X^{\dagger}$ where $\dagger$ denotes the

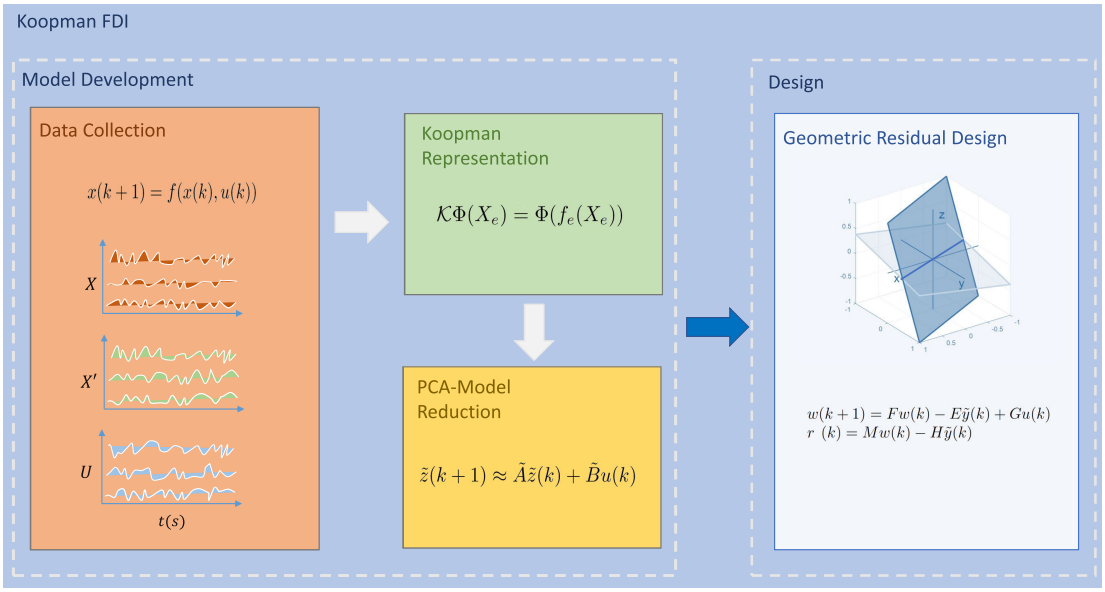

FIGURE 1. This figure presents an overview of the proposed Koopman FDI scheme. This framework mainly consists of two parts: 1. Koopman Model development, and 2. FDI observer design. To develop a model from system measurements, one needs to collect a rich dataset. Then the analogous Koopman operator of the underlying dynamics can be approximated using numerical methods such as EDMD. A PCA model reduction scheme is adopted to reduce the dimensionality of the approximated Koopman model, resulting in a Koopman-based reduced-order predictor. In the next phase, the residual generators are designed based on the obtained K-ROM using the geometric FDI approach.

Moore-Penrose pseudoinverse of a matrix. In [46], the relation between Koopman operator and DMD has been pointed out and it is shown that under the condition of having a sufficiently large set of observable functions and rich enough measurement data, DMD can be used in order to approximate a finite dimensional form of the eigen-vector and eigenvalue of the Koopman operator. By considering the set of observable functions $g_i : \mathcal{X} \to \mathbb{R},\ i = 1, \ldots, p$, and vector-valued $\boldsymbol{g}(x) = \begin{bmatrix} g_1(x) & g_2(x) & \cdots & g_p(x) \end{bmatrix}^T$, one can use EDMD which is the generalized form of the DMD and allows for the approximation of the operator $\mathcal{K}$ using arbitrary basis functions [47]. In other words, the regression is performed on an augmented vector which is containing nonlinear observable functions and this is indeed the key difference between the standard DMD and EDMD algorithms.

For the systems containing inputs, one can construct a new measurement snapshot matrix U for inputs having the form

$$U = \begin{bmatrix} u(1) & u(2) & \ldots & u(m) \end{bmatrix}, \tag{23}$$

where $U \in \mathbb{R}^{q \times m}$. Using DMDc method [48] along with the modified version of the Koopman operator introduced earlier, it is possible to decouple the effect of the actuation and obtain an approximated equivalent linear system associated with the nonlinear system (16) having the form

$$\begin{aligned} z(k+1) &\approx Az(k) + Bu(k), \\ y(k) &\approx Cz(k), \end{aligned} \tag{24}$$

where $z(k) \triangleq \boldsymbol{g}(x(k))$. Due to the high dimensionality of the system matrix, it is preferred to use a reduced order model (ROM) for designing the residual generator. One of the method to reduce the dimensionality of the matrices is the use of their projection on their POD modes instead of using the actual high dimensional matrices for evolution of our measurements [49]. The reduced order system will be defined on POD coordinate system as below

$$\tilde{z}(k+1) \approx \tilde{A}\tilde{z}(k) + \tilde{B}u(k), \tag{25}$$

where $\tilde{A}$ and $\tilde{B}$ are the reduced-order system and the control matrices, respectively. Assuming only to project our data on first $\tilde{r}$ POD modes, we get $\tilde{A} \in \mathbb{R}^{\tilde{r} \times \tilde{r}}$ and $\tilde{B} \in \mathbb{R}^{\tilde{r} \times q}$. Since it is computationally much easier to evolve the lifted dynamic on this low dimensional state, it is preferred to evolve the measurements in this space and then project them back into the high dimensional space to get the actual behavior of the system.

IV. DESIGN PROCEDURE

In this section, Koopman operator theory-based perspective toward nonlinear systems is used to obtain an affine linear model (also referred to as linear predictor) purely from data in higher dimensions which provides a global picture of the nonlinear system's behavior. Next, based on the obtained linear model, a residual generator is designed using the geometric method introduced in Section II to both detect and isolate the fault that occurred in the system. Contrary to local linearization methods, it is only needed to evaluate our model once, and it is valid globally (or at least in a large subset of the state space). It should also be noted that by a good choice of observable functions, the complete evolution of the underlying system on a lifted state space of higher dimension

(feature space) can be described using a linear operator. This paves the way for applying the methods developed for linear systems to nonlinear systems. Fig 1 depict a summary of the proposed Koopman FDI scheme.

A. MODEL DEVELOPMENT

For the construction of the model, we need to stack up some measurements and build data matrices X, X', and U defined in (21), (22), (23). By having good knowledge about the system's nonlinearity, one can choose the observable functions to lift the dynamics to a higher dimension. The lifted data matrices Z and Z' can be constructed from (21) and (22) as

$$\begin{aligned} Z &= [z(1), z(2), \ldots, z(m)], \\ Z' &= [z(2), z(3), \ldots, z(m+1)]. \end{aligned} \tag{26}$$

The matrices A and B of the linear model given by (24) can be obtained using

$$\min_{G} \parallel Z' - G\Omega \parallel_F, \tag{27}$$

where $G = [A, B]$, $\Omega = [Z^T, U^T]^T$, and $\| \cdot \|_F$ denotes the Frobenius norm of a matrix [48]. Now by considering the projection of the A and B on the first $\tilde{r}$ POD modes, the reduced-order linear model of the form (25) can be obtained. The output matrix C can be computed as the best linear estimate of X given Z, in a least-square sense by minimizing

$$\min_{C} \parallel X - CZ \parallel_F . \tag{28}$$

B. RESIDUAL DESIGN

The key part in designing the residual generator is to place the range of the fault signature that needs to be decoupled, i.e., the fault signature that the residual to be insensitive to, i.e., $\mathcal{L}_2$, in the unobservability subspace of r_1, and then factor out the unobservable subspace to achieve fault decoupling.

According to [16], by letting the $\mathcal{S}^*(\mathcal{L}_2)$ to be an unobservability subspace satisfying Theorem 1, then there exist maps $D_0 \in \underline{D}(\mathcal{S}^*)$ and H such that $\mathcal{S}^* =< \ker HC | A + D_0 C >$, where H can be obtained using $\mathrm{Ker}HC = \mathcal{S}^* + \ker C$. Let M be a unique solution of $MP = HC$, $A_0 = (A + D_0 C : \mathcal{X}/\mathcal{S}^*)$ where A_0 is the include map of $A + D_0 C$ to the quotient space $\mathcal{X}/\mathcal{S}^*$ and $P : \mathcal{X} \to \mathcal{X}/\mathcal{S}^*$ is the canonical projection satisfying $P(A + D_0 C) = A_0 P$. By construction, the pair (M, A_0) is observable, hence there exists a D_1 such that $\sigma(F) = \Lambda$, where $F = A_0 + D_1 M$, Λ is an arbitrary symmetric set, and $\sigma(F)$ denotes the spectrum of F. With P^{-r} denoting the right inverse of P, let $D = D_0 + P^{-r} D_1 H$, $E = PD$, and $G = PB$. The following detection filter generates the desired residual which is only sensitive to the fault signal f_1 and is decoupled from the fault signal f_2,

$$\begin{aligned} w(k+1) &= Fw(k) - E\tilde{y}(k) + Gu(k), \\ r_1(k) &= Mw(k) - H\tilde{y}(k). \end{aligned} \tag{29}$$

Similarly, a detection filter can be designed for detecting f_2.

Remark 1: The diagnosis accuracy of the generated residuals relies on the construction of the Koopman predictor. It is assumed that the data used to form the Koopman predictor is rich, and the bases are appropriately chosen. If the constructed predictor has high accuracy, then the generated residuals can detect and isolate the fault accurately, which leads to a low false alarm rate.

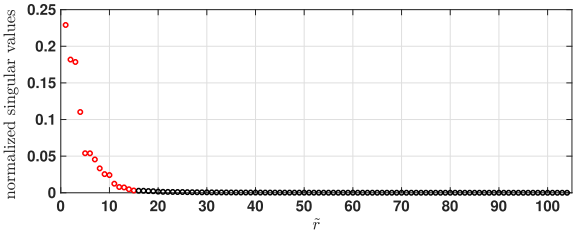

FIGURE 2. Normalized singular value spectrum of the matrix Ω. The first 15 modes are plotted in red to show the truncation order.

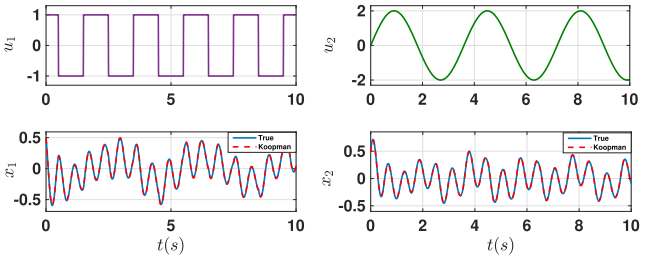

FIGURE 3. Prediction comparison between the linear reduced order model and true dynamic in case of $\tilde{r} = 15$.

V. SIMULATION AND RESULTS

A. NUMERICAL EXAMPLE

In this section, the effectiveness of the proposed K-FDI method for nonlinear systems is demonstrated. For this purpose, consider the nonlinear system of the form

$$\begin{aligned} \dot{x}_1(t) &= -10x_2(t) - x_1(t) + u_1(t), \\ \dot{x}_2(t) &= -x_2^3(t) + 10x_1(t) + u_2(t), \end{aligned} \tag{30}$$

and the system is discretized by sampling time of $T_s = 0.01$ using Runge-Kutta four method. In the data collection phase, 300 trajectories are simulated each for 10 seconds where the initial conditions and the inputs were chosen randomly with the uniform distribution on the unit box $[-1, 1]^2$ and over $[1, 1]$, respectively. The observable functions g_i are chosen as the state itself (i.e., g_1 and g_2 are x_1 and x_2, respectively), and with 100 thin plate radial basis functions with centers selected to be uniformly distributed on the unit box. A thin plate radial basis function at center c_0 is defined as

$$\|x - c_0\|^2 \log(\|x - c_0\|). \tag{31}$$

Since the proper orthogonal decomposition is an *Singular Value Decomposition (SVD)*-based method, choosing the order of truncation is of great importance. Here the simple hard thresholding is used, which is based on retaining over

the 98% of the variance in data, which leads to $\tilde{r} = 15$ to obtain a reduced-order model. Fig 2 shows the singular value spectrum resulting from the SVD of the matrix Ω. Moreover, Table 1 indicates the prediction accuracy of each ROM using root mean square error (RMSE) as a function of truncation order. It can be seen from Table 1 that the average error between the nonlinear model and the equivalent Koopman model can be reduced by choosing higher truncation order.

TABLE 1. Model validation of various Koopman reduced order model (K-ROM) using average prediction RMSE over 100 randomly chosen initial conditions as a function of truncation order.

$\tilde{r}$	5	6	10	15	20	50	102
ARMSE(x_1)	28.0%	5%	2.1%	1.8%	1.7%	1.4%	1.3%
ARMSE(x_2)	23.5%	4.9%	2.0%	1.7%	1.6%	1.33%	1.3%

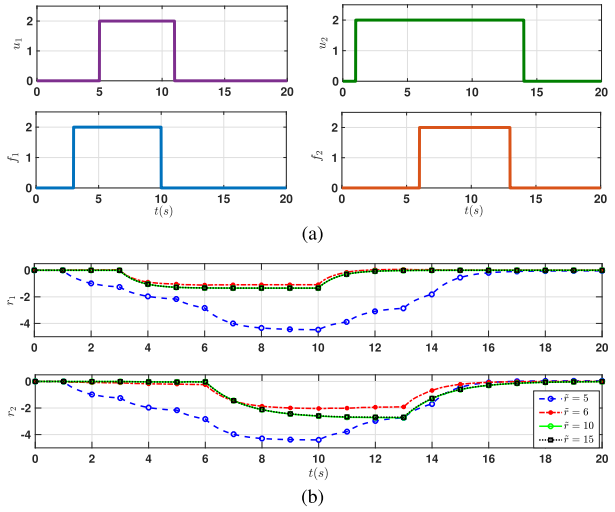

FIGURE 4. (a) The input and fault signals, (b) Generated residuals for different truncation order $\tilde{r}$.

As it is shown in Fig 3, the reduced order model perfectly follows the true dynamic. By applying the inputs u_1, u_2 and fault modes f_1 and f_2 as shown in Fig. 4a, it can be seen that r_1 and r_2 in Fig. 4b with $\tilde{r} = 15$ are only sensitive to changes of the fault modes m_1 and m_2 while they are insensitive to other system inputs. Also Fig. 4b shows that despite the fact that by reducing the system order the average RMSE increases, one can still detect and isolate both faults for $\tilde{r} \geq 6$.

B. COMPARATIVE STUDY

Since the linearization of nonlinear dynamics and the use of linear FDI techniques is by far the most common and practical approach for dealing with nonlinearities, and both Koopman-based methods and linearization-based analysis use linear techniques to solve the problem linearly; we choose to compare a data-driven linearized-based FDI method and the proposed Koopman-based FDI and illustrated the versatility of the proposed Koopman approach against the linearized-based FDI. As a comparative study, the method in [38], which performs FDI by approximating Markov parameters of the

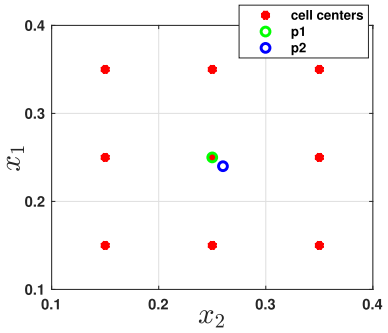

FIGURE 5. The grid showing cell centers and test operating points p1 and p2.

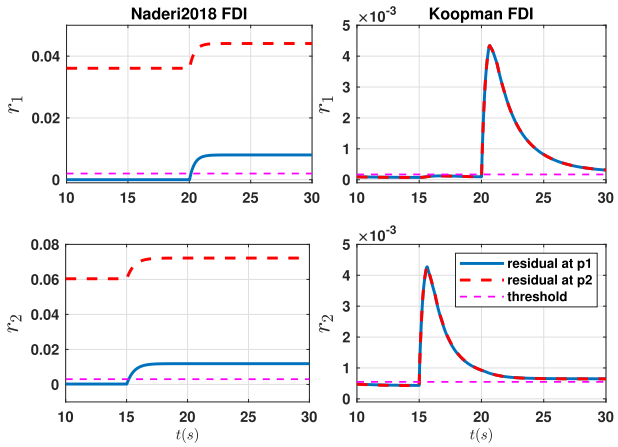

FIGURE 6. Comparison results.

system in each operating point, is used for the fault detection and isolation of the system introduced in (30). To this end, the state space is divided by 0.1×0.1 cells as it can be seen from Fig. 5 and then, a bank of residuals is designed for the center of each cell as indicated in Fig 5. In order to compare this approach with our proposed approach, consider two system operating points $p_1 = \begin{bmatrix} 0.25 & 0.25 \end{bmatrix}^T$ and $p_2 = \begin{bmatrix} 0.26 & 0.24 \end{bmatrix}^T$ which both are located in one cell. An additive fault scenario is considered where a fault with amplitude of 2 is added to $u_1(t)$ and $u_2(t)$ at $t_1 = 15s$ and $t_2 = 20s$, respectively. Fig. 6 shows that the residuals generated using the approach in [38] keep the general form by changing the operating point from p_1 to p_2 while a DC-gain is added to the residual generated at the operating point. Consequently, detection and isolation of the fault can not be properly done based on the threshold for p_2. This indeed indicates that a slight deviation from the operating points considered for the design of residual leads to false alarms. In this example, nine banks of filters were used to cover a 0.3×0.3 box in the state space and were still unable to perform FDI. The cells should be smaller to improve the method's accuracy, resulting in far more computational costs. On the contrary, residuals designed using the geometric Koopman FDI method can be applied for all

points of the considered region due to the global characteristic of the Koopman operator. In other words, The geometric Koopman FDI only needs one bank of filters for detection and isolation of the faults in the entire state space, which is far more efficient computationally.

VI. EXPERIMENTAL CASE STUDY

To illustrate the efficacy of the proposed approach, a laboratory setup of a three-tank system is considered as shown in Fig. 7a and Fig. 7b. In this study, it is assumed that the underlying dynamics are not known. Yet, it is useful to give the state equation of the system as

$$\begin{aligned} A\frac{dh_1}{dt} &= u_1 - q_{13} - q_{10}, \\ A\frac{dh_2}{dt} &= u_2 + q_{32} - q_2 - q_{20}, \\ A\frac{dh_3}{dt} &= q_{13} - q_{30} - q_{32}, \end{aligned} \tag{32}$$

where

$$\begin{aligned} q_{13} &= az_{13}S_n sgn(h_1 - h_3)\sqrt{2g|h_1 - h_3|}, \\ q_{10} &= az_{10}S_l\sqrt{2gh_1}, \\ q_{32} &= az_{32}S_n sgn(h_3 - h_2)\sqrt{2g|h_3 - h_2|}, \\ q_{30} &= az_{30}S_l\sqrt{2gh_3}, \\ q_2 &= az_2S_n\sqrt{2gh_2}, \\ q_{20} &= az_{20}S_l\sqrt{2gh_2}, \end{aligned} \tag{33}$$

and sgn$(\cdot)$ denotes the sign operator.

TABLE 2. Parameter values and descriptions for the three-tank system TTS20.

Parameter	Value/description
$h_i(t)$: liquid level of tank$_i$	ith output(m)
$u_i(t)$: flow rate of pump$_i$	ith output(m^3/s)
az_{13}: outflow coefficient between tank$_1$ and tank$_3$	1
az_{32}: outflow coefficient between tank$_3$ and tank$_2$	1
az_2 : nominal outflow coefficient of tank$_2$ to reservoir	1
az_{10}: outflow coefficient from tank$_1$ to reservoir	0
az_{20}: outflow coefficient from tank$_2$ to reservoir	0
az_{30}: outflow coefficient from tank$_3$ to reservoir	0
A: cross section of the cylinders	$0.0149(m^2)$
S_n: cross section of connection pipes	$5 \times 10^{-5}(m^2)$
S_l: cross section of circular opening pipes	$5 \times 10^{-5}(m^2)$
g: gravitation coefficient	$9.81(m/s^2)$
$u_{\min}$: lower flow rate limit of pump$_i$	$0m^3/s$
$u_{\max}$: upper flow rate limit of pump$_i$	$10^{-4}m^3/s$

The information about equations parameter and constants of the TTS20 are given in Table 2. In data collection phase, amplitude and duration of the input signals has been randomly changing within $[0, u_{\max}/1.35]$, $[0, u_{\max}]$ and $[\tau_{\min}, \tau_{\max}]$ where $\tau_{\min}$ and $\tau_{\max}$ are minimum and maximum input duration limits and chosen to be $\tau_{\min} = 1s$ and $\tau_{\max} = 170s$ by trial and error to excite all modes of the system and $u_{\max} = 10^{-4}m^3/s$. The sampling rate is selected to be $T_s = 1s$. Note that the upper limit of the first input is reduced to prevent overflow of the first tank. In order to filter out high-frequency noise components, the measured height data $(h_i, i = 1, 2, 3)$ has been passed through a low pass filter given by

$$Q(z) = \frac{1}{400z + 1}. \tag{34}$$

The observable functions g_i are chosen as the state itself with 50 thin plate radial basis functions with centers selected to be uniformly distributed in the unit cube. For the model validation, an open-loop scenario is considered where u_1 and u_2 are a repeating stair sequence with amplitude of $[0, u_{\max}/2]$ and with switching time of $1700s$ and a chirp input with initial frequency of 10^{-6} and target frequency of 3×10^{-3} with amplitude of $u_{\max}/4$ and mean of 0.55×10^{-4}, respectively. Fig. 8 shows that by applying u_1 and u_2, the obtained reduced order model with $\tilde{r} = 30$ perfectly follows the true dynamic of the three-tank system. Table 3 indicates prediction accuracy of each K-ROM with different truncation orders. In this study, two scenarios for the additive fault case, two scenarios for the leakage fault case, and two scenarios for the case of loss of effectiveness actuator fault are analyzed for a K-ROM with $\tilde{r} = 30$. It also should be noted that all faults are applied when the system has reached its steady state. To obtain steady-state tracking, two discrete-time PI controllers are designed and implemented. The values of PI controller gains are as follows: $K_{P_1} = 0.002$, $K_{I_1} = 3 \times 10^{-9}$, $K_{P_2} = 0.01$, and $K_{I_2} = 8.2 \times 10^{-6}$.

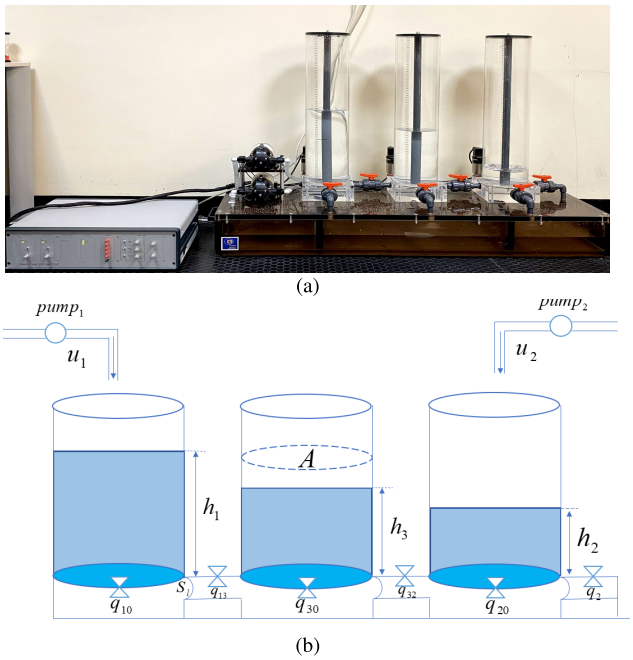

FIGURE 7. (a) Three-tank system TTS20, (b) The three-tank system TTS20 schematic.

Based on the identified K-ROM, the residuals are obtained using the geometric FDI. Since each observer produces two residuals with a non-zero offset, first, the non-zero offset of residuals is compensated by subtracting the obtained offset

TABLE 3. Model validation of various Koopman reduced order models (K-ROMs) using prediction RMSE with zero initial conditions as a function of truncation order.

$\tilde{r}$	15	20	25	30	45	53
RMSE(h_1)	14.0%	12.1%	9.4%	2.6%	1.7%	1.4%
RMSE(h_2)	8.9%	7.3%	5.9%	1.3%	1.5%	1.3%
RMSE(h_2)	10.0%	8.6%	6.9%	1.7%	1.3%	1.0%

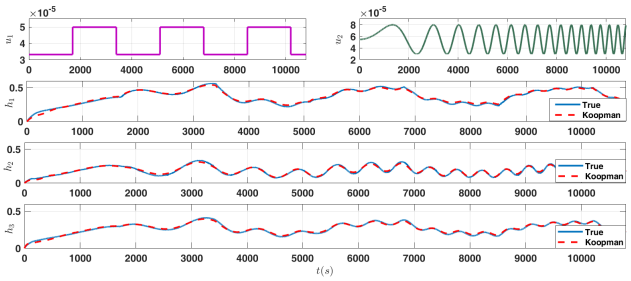

FIGURE 8. Prediction comparison between the linear reduced order model and three-tank system true dynamic in case of $\tilde{r} = 30$.

during the system's normal operation. Then norm-1 of the acquired signal is used as the residual evaluation signal.

1) ADDITIVE FAULT

In the additive fault scenario, two different cases have been tested.

CASE 1. An amount of $u_{\max}/5$ is added to u_1 during 5143s to 12000s and to u_2 during 9473s to 13846s.

CASE 2. An amount of $u_{\max}/8$ is added to u_1 during 3086s to 7200s and to u_2 during 5682s to 8307s.

An example of additive fault can be the case of having a biased regulator/controller or a biased pump in the three-tank setup.

2) LOSS OF EFFECTIVENESS ACTUATOR FAULT (LOE)

Two different cases are considered for loss of effectiveness actuator faults.

CASE 1. In this scenario, gains of pump$_1$ and pump$_2$ drops to 50% at $t_1 = 4500s$ and $t_2 = 8100s$, respectively.

CASE 2. In this scenario, gains of pump$_1$ and pump$_2$ drops to 80% at $t_1 = 4500s$ and $t_2 = 7200s$, respectively.

This type of faults can happen typically resulting from semi burnt windings in pumps.

3) LEAKAGE FAULT

Leakage fault for a tank is also considered one of the common faults occurring in tank systems by opening the leakage valve of the corresponding tank. Two different cases are then considered as follows:

CASE 1. Leakage faults are added to Tank$_1$ and Tank$_2$ by opening the leakage valve of each corresponding tank for 50% at $t_1 = 4500s$ and $t_2 = 7200s$, respectively.

CASE 2. Leakage faults are added to Tank$_1$ and Tank$_2$ by opening the leakage valve of each tank for 20% at $t_1 = 4500s$ and $t_2 = 8200s$, respectively.

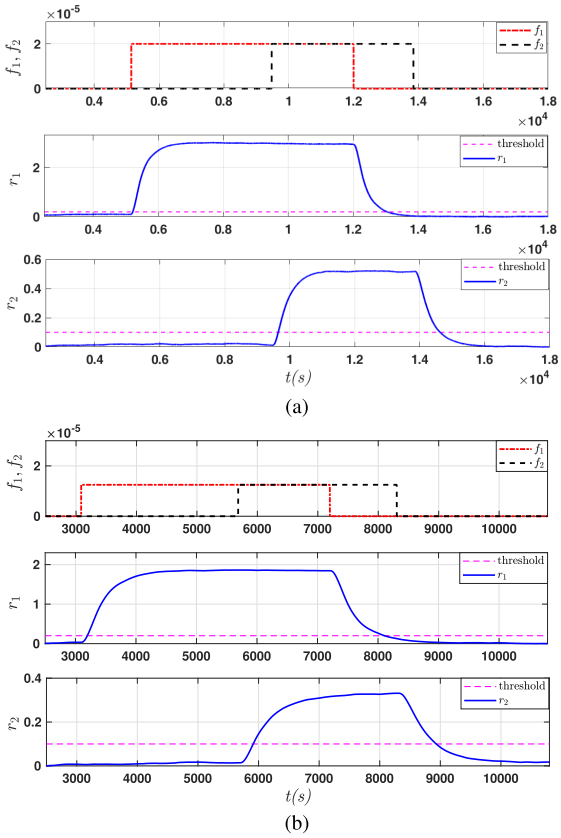

FIGURE 9. The performance of the residuals in face of the additive fault - (a) case 1, (b) case 2.

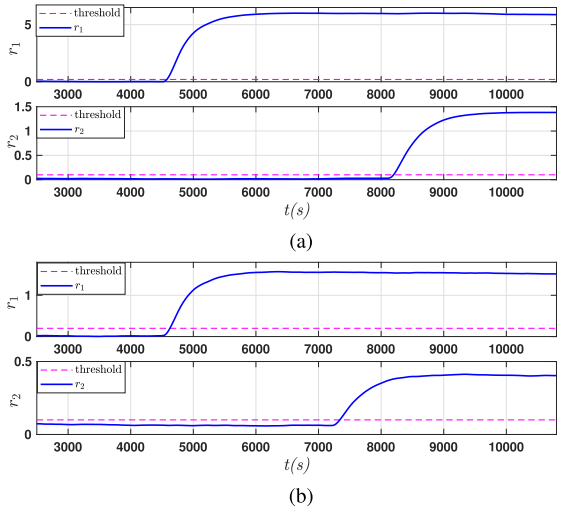

FIGURE 10. The performance of the residuals in face of the loss of effectiveness actuator fault- (a) case 1, (b) case 2.

The performance of the residuals for additive fault, loss effectiveness actuator fault, and leakage fault are presented in Figures 9 to 11, respectively. The results show that various faults can be effectively detected and isolated using the Koopman-based geometric FDI method. Table 4 shows the diagnosis time of the proposed method in each scenario. Since

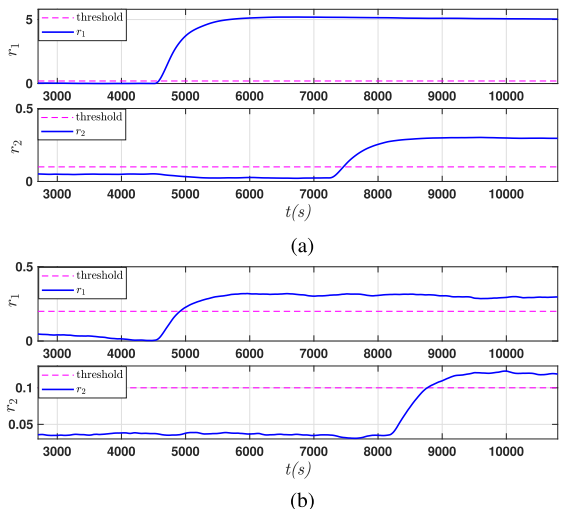

FIGURE 11. The performance of the residuals in face of the leakage fault - (a) case 1, (b) case 2.

the Three-tank benchmark has a slow dynamic, the amount of time that it takes to perform FDI by each residual, as shown in Table 4, is reasonable. The sensitivity of each residual can be increased by proper pole placement, which is useful in more severe fault scenarios.

TABLE 4. Diagnosis time of the geometric K-FDI.

		Additive		LOE		Leakage	
		case 1	case2	case 1	case2	case 1	case2
diagnosis time (min)	r_1	1	2	1	2	1	4
	r_2	3	4	2	3	3	10

It should be emphasized that none of the existing model-free FDI approaches in the literature can achieve the above performance using only healthy data as the data-driven approaches such as neural network, PCA, etc., require to have faulty data for fault isolation. In contrast, model identification methods such as [38] require obtaining the linearized model of the system at different operating points. As shown in the previous example, a slight deviation from these operating points leads to false alarms. However, the proposed Koopman-based FDI does not have any of the above weaknesses and can be utilized for fault detection and isolation using the available healthy data from the system.

VII. CONCLUSION

This paper presents a data-driven method for fault detection and isolation of the nonlinear dynamical systems by integrating Koopman-based system identification within a linear geometric FDI framework. The key idea is to use the Koopman operator for obtaining a meaningful, linear representation of the underlying (nonlinear) dynamical system, which is valid *globally* and captures the inherent properties of the system. A finite-dimensional approximation of the Koopman operator yields a linear model, which uses model-based analytical FDI techniques. Specifically, we proposed using a reduced order form of the Koopman-based linear model in combination with the geometric approach to the FDI problem of nonlinear systems. Case study results are presented to illustrate the effectiveness of the proposed method.

REFERENCES

[1] J. Chen and R. J. Patton, *Robust Model-Based Fault Diagnosis for Dynamic Systems*, vol. 3. New York, NY, USA: Springer, 2012.
[2] M. Thirumarimurugan, N. Bagyalakshmi, and P. Paarkavi, "Comparison of fault detection and isolation methods: A review," in *Proc. 10th Int. Conf. Intell. Syst. Control (ISCO)*, Jan. 2016, pp. 1–6.
[3] M. Alauddin, F. Khan, S. Imtiaz, and S. Ahmed, "A bibliometric review and analysis of data-driven fault detection and diagnosis methods for process systems," *Ind. Eng. Chem. Res.*, vol. 57, no. 32, pp. 10719–10735, 2018.
[4] N. Meskin and K. Khorasani, "Actuator fault detection and isolation for a network of unmanned vehicles," *IEEE Trans. Autom. Control*, vol. 54, no. 4, pp. 835–840, Apr. 2009.
[5] N. Meskin, E. Naderi, and K. Khorasani, "A multiple model-based approach for fault diagnosis of jet engines," *IEEE Trans. Control Syst. Technol.*, vol. 21, no. 1, pp. 254–262, Jan. 2013.
[6] N. Meskin and K. Khorasani, *Fault Detection and Isolation: Multi-Vehicle Unmanned Systems*. New York, NY, USA: Springer, 2011.
[7] R. H. Chen, D. L. Mingori, and J. L. Speyer, "Optimal stochastic fault detection filter," *Automatica*, vol. 39, no. 3, pp. 377–390, Mar. 2003.
[8] L. Berec, "A multi-model method to fault detection and diagnosis: Bayesian solution. An introductory treatise," *Int. J. Adapt. Control Signal Process.*, vol. 12, no. 1, pp. 81–92, Feb. 1998.
[9] J. Chen and H.-Y. Zhang, "Parity vector approach for detecting failures in dynamic systems," *Int. J. Syst. Sci.*, vol. 21, no. 4, pp. 765–770, Apr. 1990.
[10] P. M. Frank, "Fault diagnosis in dynamic systems using analytical and knowledge-based redundancy: A survey and some new results," *Automatica*, vol. 26, no. 3, pp. 459–474, 1990.
[11] X. Zhang, M. M. Polycarpou, and T. Parisini, "Fault diagnosis of a class of nonlinear uncertain systems with Lipschitz nonlinearities using adaptive estimation," *Automatica*, vol. 46, no. 2, pp. 290–299, 2010.
[12] W. Chen and M. Saif, "Fault detection and isolation based on novel unknown input observer design," in *Proc. Amer. Control Conf.*, 2006, pp. 1–6.
[13] V. Krishnaswami and G. Rizzoni, "Nonlinear parity equation residual generation for fault detection and isolation," *IFAC Proc. Volumes*, vol. 27, no. 5, pp. 305–310, Jun. 1994.
[14] Y. Jiang, S. Yin, and O. Kaynak, "Optimized design of parity relation-based residual generator for fault detection: Data-driven approaches," *IEEE Trans. Ind. Informat.*, vol. 17, no. 2, pp. 1449–1458, Feb. 2021.
[15] X.-G. Yan and C. Edwards, "Nonlinear robust fault reconstruction and estimation using a sliding mode observer," *Automatica*, vol. 43, no. 9, pp. 1605–1614, 2007.
[16] M.-A. Massoumnia, G. C. Verghese, and A. S. Willsky, "Failure detection and identification," *IEEE Trans. Autom. Control*, vol. 34, no. 3, pp. 316–321, Mar. 1989.
[17] N. Meskin and K. Khorasani, "Fault detection and isolation of distributed time-delay systems," *IEEE Trans. Autom. Control*, vol. 54, no. 11, pp. 2680–2685, Nov. 2009.
[18] N. Meskin and K. Khorasani, "A geometric approach to fault detection and isolation of continuous-time Markovian jump linear systems," *IEEE Trans. Autom. Control*, vol. 55, no. 6, pp. 1343–1357, Jun. 2010.
[19] J. Bokor and G. Balas, "Detection filter design for LPV systems—A geometric approach," *Automatica*, vol. 40, no. 3, pp. 511–518, Mar. 2004.
[20] N. Meskin and K. Khorasani, "Fault detection and isolation of linear impulsive systems," *IEEE Trans. Autom. Control*, vol. 56, no. 8, pp. 1905–1910, Aug. 2011.
[21] N. Meskin and K. Khorasani, "Robust fault detection and isolation of time-delay systems using a geometric approach," *Automatica*, vol. 45, no. 6, pp. 1567–1573, Jun. 2009.
[22] A. Baniamerian, N. Meskin, and K. Khorasani, "A geometric approach to fault detection and isolation of multi-dimensional (n-D) systems," *Multidimensional Syst. Signal Process.*, vol. 28, no. 4, pp. 1653–1678, Oct. 2017.
[23] A. Baniamerian and K. Khorasani, "Fault detection and isolation of dissipative parabolic PDEs: Finite-dimensional geometric approach," in *Proc. Amer. Control Conf. (ACC)*, Jun. 2012, pp. 5894–5899.

[24] C. De Persis and A. Isidori, "A geometric approach to nonlinear fault detection and isolation," *IEEE Trans. Autom. Control*, vol. 46, no. 6, pp. 853–865, Jun. 2001.
[25] H. R. Patel and V. A. Shah, "Fault detection and diagnosis methods in power generation plants—The Indian power generation sector perspective: An introductory review," *PDPU J. Energy Manage.*, vol. 2, no. 2, pp. 31–49, 2018.
[26] X. Dai and Z. Gao, "From model, signal to knowledge: A data-driven perspective of fault detection and diagnosis," *IEEE Trans. Ind. Informat.*, vol. 9, no. 4, pp. 2226–2238, Nov. 2013.
[27] C. Alippi, S. Ntalampiras, and M. Roveri, "Model-free fault detection and isolation in large-scale cyber-physical systems," *IEEE Trans. Emerg. Topics Comput. Intell.*, vol. 1, no. 1, pp. 61–71, Feb. 2017.
[28] S. Rajakarunakaran, P. Venkumar, D. Devaraj, and K. S. P. Rao, "Artificial neural network approach for fault detection in rotary system," *Appl. Soft Comput.*, vol. 8, no. 1, pp. 740–748, Jan. 2008.
[29] D. J. Bordoloi and R. Tiwari, "Support vector machine based optimization of multi-fault classification of gears with evolutionary algorithms from time–frequency vibration data," *Measurement*, vol. 55, pp. 1–14, Sep. 2014.
[30] S. Klus, F. Nüske, S. Peitz, J.-H. Niemann, C. Clementi, and C. Schütte, "Data-driven approximation of the Koopman generator: Model reduction, system identification, and control," *Phys. D, Nonlinear Phenomena*, vol. 406, May 2020, Art. no. 132416.
[31] B. Chen, Z. Huang, R. Zhang, W. Liu, H. Li, J. Wang, Y. Fan, and J. Peng, "Data-driven Koopman model predictive control for optimal operation of high-speed trains," *IEEE Access*, vol. 9, pp. 82233–82248, 2021.
[32] S. Xie and J. Ren, "Linearization of recurrent-neural-network- based models for predictive control of nano-positioning systems using data-driven Koopman operators," *IEEE Access*, vol. 8, pp. 147077–147088, 2020.
[33] X. Li, J. De La Ree, and C. Mishra, "Frequency control of decoupled synchronous machine using Koopman operator based model predictive," in *Proc. IEEE Power Energy Soc. Gen. Meeting (PESGM)*, Aug. 2019, pp. 1–5.
[34] D. Bruder, X. Fu, R. B. Gillespie, C. D. Remy, and R. Vasudevan, "Data-driven control of soft robots using Koopman operator theory," *IEEE Trans. Robot.*, vol. 37, no. 3, pp. 948–961, Jun. 2021.
[35] C. Cheng, J. Ding, and Y. Zhang, "A Koopman operator approach for machinery health monitoring and prediction with noisy and low-dimensional industrial time series," *Neurocomputing*, vol. 406, pp. 204–214, Sep. 2020.
[36] A. Surana, "Koopman operator framework for time series modeling and analysis," *J. Nonlinear Sci.*, vol. 30, no. 5, pp. 1973–2006, Oct. 2020.
[37] S. Peitz and S. Klus, "Koopman operator-based model reduction for switched-system control of PDEs," *Automatica*, vol. 106, pp. 184–191, Aug. 2019.
[38] E. Naderi and K. Khorasani, "Data-driven fault detection, isolation and estimation of aircraft gas turbine engine actuator and sensors," *Mech. Syst. Signal Process.*, vol. 100, pp. 415–438, Feb. 2018.
[39] M. Korda and I. Mezić, "Linear predictors for nonlinear dynamical systems: Koopman operator meets model predictive control," *Automatica*, vol. 93, pp. 149–160, Jul. 2018.
[40] W. Li, M. Peng, and Q. Wang, "Improved PCA method for sensor fault detection and isolation in a nuclear power plant," *Nucl. Eng. Technol.*, vol. 51, no. 1, pp. 146–154, Feb. 2019.
[41] R. Iqbal, T. Maniak, F. Doctor, and C. Karyotis, "Fault detection and isolation in industrial processes using deep learning approaches," *IEEE Trans. Ind. Informat.*, vol. 15, no. 5, pp. 3077–3084, May 2019.
[42] G. Basile and G. Marro, *Controlled and Conditioned Invariants in Linear System Theory*. Englewood Cliffs, NJ, USA: Prentice-Hall, 1992.
[43] M.-A. Massoumnia, "A geometric approach to the synthesis of failure detection filters," *IEEE Trans. Autom. Control*, vol. AC-31, no. 9, pp. 839–846, Sep. 1986.
[44] S. L. Brunton, B. W. Brunton, J. L. Proctor, and J. N. Kutz, "Koopman invariant subspaces and finite linear representations of nonlinear dynamical systems for control," *PLoS ONE*, vol. 11, no. 2, Feb. 2016, Art. no. e0150171.
[45] T. H. Jonathan, C. W. Rowley, D. M. Luchtenburg, S. L. Brunton, and J. N. Kutz, "On dynamic mode decomposition: Theory and applications," *J. Comput. Dyn.*, vol. 1, no. 2, pp. 391–421, 2014.
[46] C. W. Rowley, I. Mezić, S. Bagheri, P. Schlatter, and D. S. Henningson, "Spectral analysis of nonlinear flows," *J. Fluid Mech.*, vol. 641, pp. 115–127, Dec. 2009.
[47] S. Klus, P. Koltai, and C. Schütte, "On the numerical approximation of the Perron–Frobenius and koopman operator," *J. Comput. Dyn.*, vol. 3, pp. 51–79, Sep. 2016.
[48] J. L. Proctor, S. L. Brunton, and J. N. Kutz, "Dynamic mode decomposition with control," *SIAM J. Appl. Dyn. Syst.*, vol. 15, no. 1, pp. 142–161, 2016.
[49] M. Mrosek, C. Othmer, and R. Radespiel, "Reduced-order modeling of vehicle aerodynamics via proper orthogonal decomposition," *SAE Int. J. Passenger Cars-Mech. Syst.*, vol. 12, no. 3, pp. 225–236, Oct. 2019.

MOHAMMADHOSEIN BAKHTIARIDOUST was born in Qom, Iran, in 1997. He received the B.Sc. degree in control engineering from the Qom University of Technology, Qom, in 2019, where he is currently pursuing the M.Sc. degree in control engineering. His research interests include data-driven control, fault detection and isolation, and machine learning.

MEYSAM YADEGAR received the B.Sc. degree from the Sahand University of Technology, Tabriz, Iran, in 2006, the M.Sc. degree from the K. N. Toosi University of Technology, Tehran, Iran, in 2010, and the Ph.D. degree from the Amirkabir University of Technology, Tehran, in 2017, all in control engineering. He is currently an Assistant Professor at the Qom University of Technology, Qom, Iran. His research interests include FTC, multi-agent systems, and nonlinear control.

NADER MESKIN (Senior Member, IEEE) received the B.Sc. degree from the Sharif University of Technology, Tehran, Iran, in 1998, the M.Sc. degree from the University of Tehran, Tehran, in 2001, and the Ph.D. degree in electrical and computer engineering from Concordia University, Montreal, QC, Canada, in 2008. He was a Postdoctoral Fellow at Texas A&M University at Qatar, Doha, Qatar, from January 2010 to December 2010. He is currently a Professor at Qatar University, Doha, and an Adjunct Associate Professor at Concordia University. He has published more than 250 refereed journal and conference papers. His research interests include FDI, multiagent systems, active control for clinical pharmacology, cyber-security of industrial control systems, and linear parameter varying systems.

MOHAMMAD NOORIZADEH received the B.Sc. degree from Qatar University, Doha, Qatar, in 2015. He has been a Research Assistant at Qatar University, since 2015. His research interests include machine learning, automation, control, and robotics.